

# Tracing Hierarchical Cloud–Cloud Collisions with High-Density Molecular Lines

## 1 Scientific Justification

### 1.1 Scientific rationale:

Stars form via the gravitational collapse of dense gas in molecular clouds. Massive stars, in particular, are known to form only in clusters within giant molecular clouds (GMCs), but the mechanisms linking GMCs to cluster formation remain unclear. Although star formation is influenced by large-scale galactic structures like spiral arms, how these affect the local environment of molecular clouds is not well understood.

Recent observations have frequently reported signs of cloud–cloud collisions (CCCs) in massive star-forming regions. For example, FUGIN data from the Nobeyama 45m telescope[1] have revealed at least four velocity components interacting near W51A[2] (Figure 1), suggesting possible CCCs. However, estimates indicate that the timescale for such collisions is longer than that for cloud collapse, implying CCCs may not dominate massive star formation[3].

By analyzing both FUGIN data and hydrodynamical simulations with Dendrograms[4], we propose a new scenario: GMCs contract globally while dense substructures form hierarchically and frequently collide, eventually triggering massive star formation (Figure 2). This scenario naturally produces repeated internal collisions during global collapse, offering a unified explanation for why massive stars form only in GMCs and why CCCs are commonly seen near such regions. While this is consistent with hierarchical collapse models[5][6], our work is the first to test this using high-resolution data and uniform Dendrogram analysis.

However, CO-based Dendrograms alone cannot confirm whether gas dense enough for star formation actually results from these hierarchical CCCs. To test this, molecular line observations sensitive to higher densities are required.

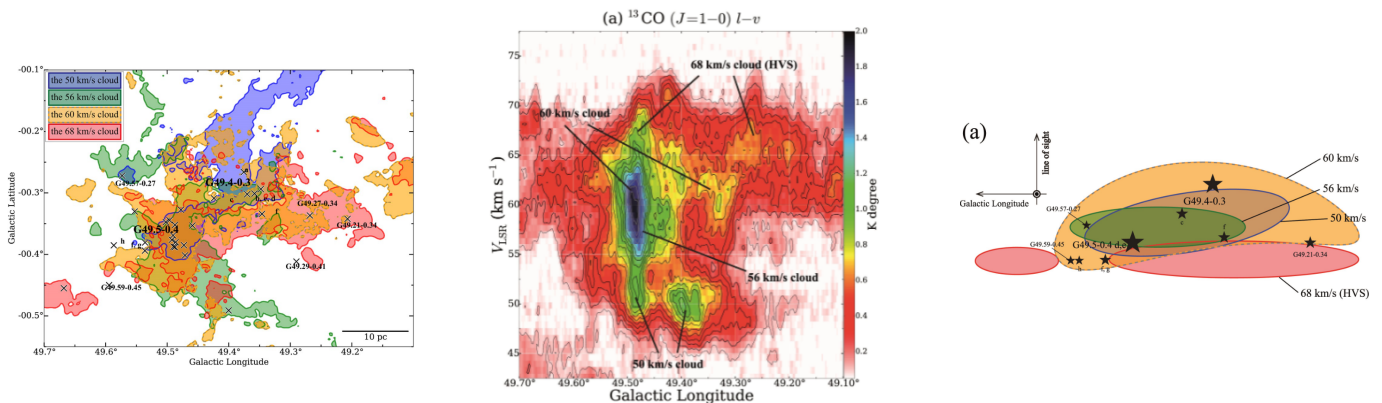


Figure 1: (Left)  $^{13}\text{CO}$  ( $J = 1-0$ ) integrated intensity distributions of the clouds of various velocities in W51A. The crosses represent Hii regions listed by Mehringer (1994). (Center) Galactic latitude–velocity ( $l-v$ ) diagram of the  $^{13}\text{CO}$  ( $J = 1-0$ ) emissions integrated over  $b = -0^\circ.55$ – $-0^\circ.10$  in W51A. (Right) Schematic pictures of the distributions of the molecular gas in W51A as viewed from the Galactic north pole. The star markers indicate the positions of the representative HII regions in W51A. The presence of molecular clouds with multiple velocity components and the location of HII regions at their boundaries suggest that massive star formation in W51A is triggered by cloud–cloud collisions (CCCs). All panels are adapted from Fujita et al. (2021).

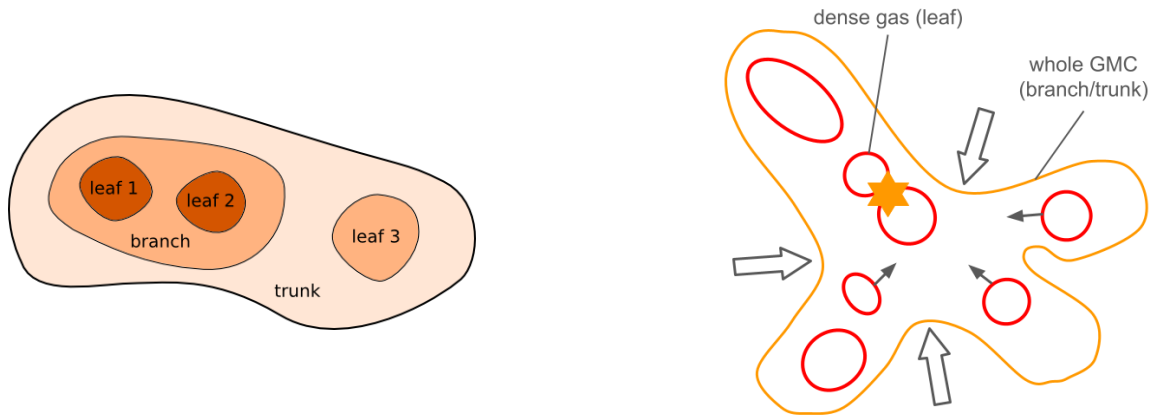


Figure 2: (Right) Schematic of hierarchical structures identified by Dendrogram analysis. Dendrograms decompose data into leaves (innermost, densest structures), branches (encompassing leaves), and the outermost trunk. In molecular line data, leaves represent the densest gas components forming the hierarchical structure. (Left) Schematic of hierarchical CCCs. Large-scale structures (trunks and branches) undergo global contraction, while dense substructures (leaves) form hierarchically and frequently collide. These collisions ultimately trigger massive star formation.

## 1.2 Immediate objective:

In this study, we propose follow-up observations using the high-density tracers HCN ( $J = 1-0$ ) and  $\text{HCO}^+$  ( $J = 1-0$ ) to investigate the spatial distribution and kinematic properties of dense gas within the hierarchical structures identified from the FUGIN CO data. This will allow us to test whether hierarchical gravitational collapse is promoting interactions among dense structures that can lead to massive star formation.

The HCN ( $J = 1-0$ ) and  $\text{HCO}^+$  ( $J = 1-0$ ) lines trace gas with typical critical densities of  $\sim 4.7 \times 10^5 \text{ cm}^{-3}$  and  $\sim 6.8 \times 10^4 \text{ cm}^{-3}$  at 10 K, respectively[7]. When combined with CO ( $J = 1-0$ ) data, which trace the gas at  $\sim 10^3 \text{ cm}^{-3}$ , these lines serve as a stepwise probe of the gas density across several orders of magnitude. Observing both HCN and  $\text{HCO}^+$  simultaneously, we can examine how dense gas emerges from the diffuse envelope traced by CO and condenses into compact, potentially star-forming structures, providing a continuous, multilayered view of the internal structure of the cloud.

In this proposal, we focus on the W51A region, which exhibits multiple velocity components in the CO data. In W51A, dense gas structures corresponding to individual velocity components have been identified as Dendrogram leaves, whereas the encompassing trunks extend across multiple velocity ranges. This configuration strongly suggests the presence of hierarchical cloud–cloud collisions within a globally collapsing GMC. W51A is therefore an ideal candidate for probing whether such interactions actually give rise to massive star-forming structures and for testing the hypothesized connection between hierarchical structure and star-formation activity.

Particular attention in the analysis will be given to regions where multiple velocity components overlap and where individual Dendrogram leaves meet at the interface, as these sites may represent collision fronts formed within the hierarchical framework. Confirming the presence of dense gas condensations in these regions would provide direct evidence that hierarchical CCCs mediated by global gravitational collapse are actively producing the seeds of massive stars.

If the presence of dense condensations is confirmed in the proposed regions, it will pave the way for the next step: high-resolution follow-up observations with ALMA (Atacama Large Millimeter/submillimeter Array). Building on the results of this study, which will characterize the global distribution and kinematics of dense gas, ALMA’s superior resolution and sensitivity will allow us to examine the internal structures of the identified structures in much greater detail. By linking the cloud-scale dynamics with the core-scale physical processes revealed by ALMA observations, this multi-scale approach will enable a more comprehensive test of the proposed hierarchical gravitational collapse scenario.

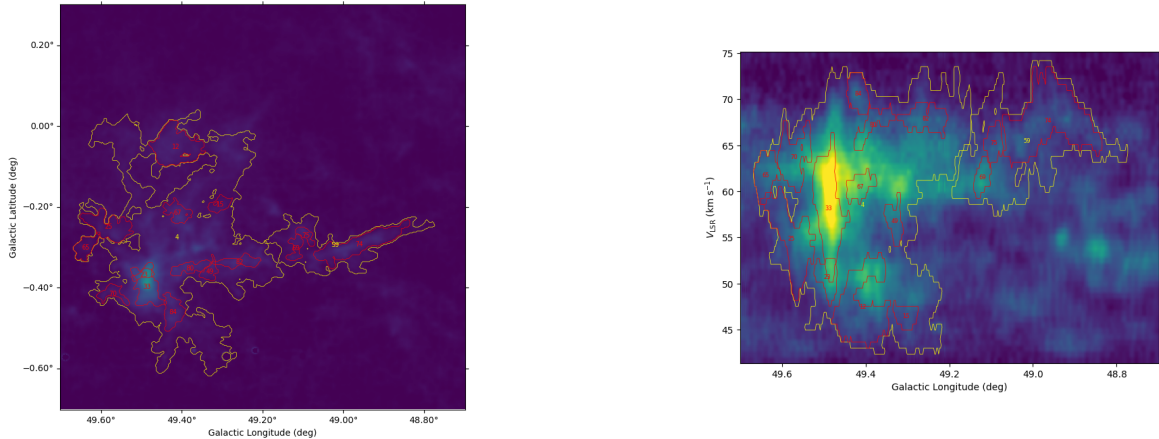


Figure 3: (Right) Selected structures identified by Dendrogram analysis of the  $^{13}\text{CO}$  molecular line data of W51A, overlaid on the moment 0 map. Larger structures, outlined in yellow contours, can be seen surrounding the denser structures outlined in red. (Left) Same as right panel, but overlaid on the  $l$ - $v$  diagram.

## 2 Observation Plan

We will observe the W51A region, defined as  $l = 49.2\text{--}49.6^\circ$ ,  $b = -0.6\text{--}0.0^\circ$  in Galactic coordinates, targeting two molecular lines: HCN ( $J = 1 - 0$ , 88.631847 GHz) and  $\text{HCO}^+$  ( $J = 1 - 0$ , 89.188525 GHz). The observations will be carried out with the FOREST receiver and the SAM45 spectrometer on the Nobeyama 45-m telescope. The velocity resolution is set to  $0.65 \text{ km s}^{-1}$ , matching the FUGIN CO data for direct comparison of kinematic structure.

To estimate the required integration time, we used the average peak temperature ratios of CO to HCN and  $\text{HCO}^+$  derived from previous observations of M17 (Pérez-Beaupuits et al. 2015). Specifically, we adopted  $\text{HCN}/\text{CO} = 6.51/30.66 \approx 0.21$  and  $\text{HCO}^+/\text{CO} = 6.28/30.66 \approx 0.20$ , based on the average spectra in M17. Using these ratios, we estimated the expected peak temperatures of HCN and  $\text{HCO}^+$  for W51A, and calculated the integration time required to achieve a signal-to-noise ratio of  $5\sigma$ . The total on-source integration time, after accounting for a  $1.3\times$  overhead for tuning, pointing, and calibration, is estimated to be 52.3 hours. As HCN and  $\text{HCO}^+$  will be observed simultaneously, this integration time applies to both lines.

## 3 References

- [1] Umemoto T., et al. 2017, *PASJ*, 69, 5
- [2] Fujita S., et al. 2021, *PASJ*, 73, S172
- [3] Sun J., et al. 2022, *ApJ*, 164, 43
- [4] Rosolowsky E. W., et al. 2008, *ApJ*, 679, 1338
- [5] Ballesteros-Paredes J., et al. 2011, *MNRAS*, 411, 1
- [6] Vázquez-Semadeni E., et al. 2019, *MNRAS*, 490, 3
- [7] Shirley Y. L., et al. 2015, *PASP*, 127, 299
- [8] Pérez-Beaupuits J.P., et al. 2015, *A&A*, 583, A107